Hydrogen Cyanide Accumulation and Transformations in Non-polluted Salt Marsh Sediments

Citation: Kamyshny, A., H. Oduro, Z. F. Mansaray, and J. Farquhar. "Hydrogen Cyanide Accumulation and Transformations in Non-Polluted Salt Marsh Sediments." Aquat Geochem 19, no. 2 (October 13, 2012): 97–113.

As Published: http://dx.doi.org/10.1007/s10498-012-9180-5

Publisher: Springer Netherlands

Persistent URL: http://hdl.handle.net/1721.1/105832

Version: Author's final manuscript: final author's manuscript post peer review, without publisher's formatting or copy editing

Aquat Geochem (2013) 19:97–113
DOI 10.1007/s10498-012-9180-5

ORIGINAL PAPER

Hydrogen Cyanide Accumulation and Transformations in Non-polluted Salt Marsh Sediments

A. Kamyshny Jr. · H. Oduro · Z. F. Mansaray · J. Farquhar

Received: 23 April 2012 / Accepted: 3 October 2012 / Published online: 13 October 2012

Abstract While cyanide is known to be produced by many organisms, including plants, bacteria, algae, fungi and some animals, it is generally thought that high levels of cyanide in aquatic systems require anthropogenic sources. Here, we report accumulation of relatively high levels of cyanide in non-polluted salt marsh sediments (up to 230 μmol kg^{-1}). Concentrations of free cyanide up to 1.92 μmol L^{-1}, which are toxic to aquatic life, were detected in the pore-waters. Concentration of total (free and complexed) cyanide in the pore-waters was up to 6.94 μmol L^{-1}. Free cyanide, which is released to the marsh sediments, is attributed to processes associated with decomposition of cord grass, *Spartina alterniflora,* roots and possibly from other sources. This cyanide is rapidly complexed with iron and adsorbed on sedimentary organic matter. The ultimate cyanide sink is, however, associated with formation of thiocyanate by reaction with products of sulfide oxidation by Fe(III) minerals, especially polysulfides. The formation of thiocyanate by this pathway detoxifies two poisonous compounds, polysulfides and hydrogen cyanide, preventing release of free hydrogen cyanide from salt marsh sediments into overlying water or air.

Keywords Hydrogen cyanide · Metallo-cyanide complexes · Thiocyanate
Sulfide oxidation intermediates · Inorganic polysulfides · Sulfide

A. Kamyshny Jr. · H. Oduro · Z. F. Mansaray · J. Farquhar
Department of Geology and Earth Systems Science Interdisciplinary Center, University of Maryland, College Park, MD 20742, USA

A. Kamyshny Jr.
Department of Biogeochemistry, Max Planck Institute for Marine Microbiology, Celsuisstrasse 1, 28359 Bremen, Germany

A. Kamyshny Jr. (✉)
Department of Geological and Environmental Sciences, Faculty of Natural Sciences, Ben-Gurion University of the Negev, P.O. Box 653, 84105 Beer Sheva, Israel
e-mail: alexey93@gmail.com

H. Oduro
Department of Earth, Atmospheric, and Planetary Sciences (EAPS), Massachusetts Institute of Technology, 77 Massachusetts Avenue, Cambridge, MA 02139, USA

1 Introduction

Cyanide and its protonated form, HCN, are important anthropogenic pollutants of natural aquatic systems (Young et al. 2006; Ghosh et al. 2006a). Cyanide discharges from gold mine heap leaching operations such as those that occurred at the USMX mine, Utah, USA in 1995, which released 26,000 m^3 of 0.2 ppm cyanide solution to East Fork of Beaver Dam Wash, or at Omai, Guyana in 1995, at the Gold Quarry mine, Nevada, USA in 1997, and at Baia Mare, Romania in 2000 have had a profound influence on riverine systems (Wong-Chong et al. 2006a). Cyanide is lethal at concentrations in the range of 1–40 μmol L^{-1} for fish and 3–1,920 μmol L^{-1} for invertebrate organisms (LC50, 96-h exposure) (Gensemer et al. 2006), and cyanide spills are known to result in massive fish kills (Wong-Chong et al. 2006a).

Significant cyanide accumulation due to natural processes in marine systems has not however been reported (Wong-Chong et al. 2006b), and its low concentrations are attributed to fast uptake (and degradation) by plants, fungi and bacteria in aquatic systems, as well as volatilization and adsorption (Yu et al. 2005; Ghosh et al. 2006b). Bacteria and fungi are known to degrade cyanide (Ghosh et al. 2006b). It turns out the atmospheric cyanide produced by biomass burning is the main source of cyanide to the ocean. Estimates by Li et al. (2000) attribute a release of 1.4–2.9 Tg N per year to the atmosphere due to forest fires. In lake waters, for instance, up to 0.65 μmol L^{-1} and 1.85 μmol L^{-1} of free and total cyanide, respectively, has been detected by potentiometry (Sekerka and Lechner 1976). Its concentration in upper ocean waters is likely less than $\sim$40 nmol L^{-1}, but no direct measurements are available (Li et al. 2000; Dzombak et al. 2006a). Concentrations of cyanide may be higher in coastal waters affected by wastewater discharge or "cyanide fishing" (Dzombak et al. 2006a).

Natural sources of cyanide include production by various organisms, including bacteria, fungi and especially vascular plants. A well-documented case is production of cyanide by the important food plant *Manihot esculenta* (cassava) (Wong-Chong et al. 2006b; Ghosh et al. 2006b). Numerous plants can use cyanide as a source of nitrogen, but they are also not immune to its effects as an inhibitor of respiratory metabolic processes. Cyanide is also known to inhibit microbial denitrification and methanogenesis (Wild et al. 1994).

Here, we report an observation of accumulation of high concentrations of cyanide in salt marsh sediment of the Delaware Great Marsh (DGM), a system that is not affected by significant anthropogenic sources of cyanide and that was not expected to hold this compound in its various forms at high levels.

The DGM is a salt marsh, dominated by *Spartina alterniflora* (saltmarsh cordgrass) and has an active annual cycle of sulfur and iron (Lord et al. 1983; Luther et al. 1986; Ferdelman et al. 1991; Luther et al. 1991; Kostka and Luther 1994, 1995). From mid-summer to mid-spring, the iron-sulfide transition zone in the pore-waters is relatively shallow (at 0–10 cm depth). Sulfide accumulates below the iron-sulfide transition zone in sediments due to microbial sulfate reduction resulting in the formation of pyrite. From the mid-spring to mid-summer, penetration of oxygen through growing and hollow dead *Spartina alterniflora* roots causes deepening of the iron-sulfide transition zone to 10–20 cm, and pyrite oxidation occurs above this level (Luther et al. 1991). Oxidation of sulfide and pyrite by iron(III) leads to the formation of sulfate and a variety of sulfide oxidation intermediates, such as inorganic polysulfides (S_n^{2-}) and their protonated forms, thiosulfate, sulfite, tetrathionate and thiols (Luther et al. 1986). In late summer and autumn, sulfate reduction rates (and therefore rates of organic matter decomposition) are relatively high and reducing conditions prevail in sediments. The upper layer of the solid phase of the

DGM sediments (2.5 cm) is dominated by Fe(III) (amorphous and crystalline) around the year, except late summer—early autumn, when sulfur bound iron (especially pyrite) comprises half or more of all iron. The fraction of sulfur bound iron increases with depth and dominates vegetated salt marsh sediments at 20–25 cm depth around the year (Kostka and Luther 1995). Solid phase sulfur is bound to iron as iron sulfide. Pyrite sulfur usually prevails over other iron-sulfide minerals, especially in the deep sediments (Kostka and Luther 1995), although sometimes in the upper 2.5 cm of sediment, pyrite sulfur may comprise less than 50 % of solid sediment sulfur pool (Kostka and Luther 1994).

In salt marshes, cyanogenic glycoside triglochinin (Ettlinger and Eyjólfsson 1972) is known to be produced by arrowgrass (*Triglochin maritima*) (Majak et al. 1980; Davy and Bishop 1991). The highest content of triglochinin was detected in new growth of leaves and spikes of *Triglochin maritima* in spring. No published data on cyanogenic potential of *Spartina alterniflora* were found.

The main goal of the performed research was to understand sources of high cyanide content in the Delaware Great Marsh sediments as well as pathways of cyanide transformations, and its temporary and permanent sinks.

2 Materials and Methods

2.1 Sampling and Core Processing

Samplings were performed on October 30, 2009 and on April 14, 2010. The sampling site was located in the Delaware Great Marsh (DGM) at the southern shore of the Delaware Bay near Lewes, DE (38°48′N, 75°12′W) at the shore of a small creek. The site was dominated by *Spartina alterniflora* grass. A detailed site description may be found in the work of Luther et al. (1991).

During each sampling, three cores were taken. The first core was used for pore-water extraction and analysis. The second core was used for a bulk sediment analysis, and the third core was used for incubations of amended sediment slurry. During both sampling campaigns, all cores were taken not more than 3 m from the same reference point in the vicinity of creek. Cores were retrieved by pushing 9.5-cm–internal diameter, 50-cm-long polycarbonate liner with a sharpened lower edge into the marsh sediment. All depths are reported as they were sampled from the core liner. Sediment compaction during sampling was 5–7 % of core length.

The pore-water was extracted with Rhizon samplers (MacroRhizon, 9 cm long, 4.5 mm diameter, Rhizosphere Research Products, Netherlands) with a filter pore size of 100 nm, under a nitrogen atmosphere in the glove box (typically <0.2 % O_2). The Rhizon samplers were horizontally inserted in the cores through predrilled holes that had been sealed with gas-tight tape before sampling. After insertion, the Rhizon samplers were connected to syringes which were used to create a small amount of underpressure. Prior to pore-water extraction, the Rhizon samplers were stored for at least one hour in anoxic water in the glove box. Syringes were flushed several times with the glove box atmosphere before they were attached to the Rhizon samplers. The first milliliter of the extracted pore-water was discarded to avoid contamination from oxygen absorbed on the Rhizon samplers and/or syringe plunger, and the dilution of seawater sample with anoxic Milli-Q in which the Rhizons were stored. Usually, c.a. 20–30 mL of pore-water was sampled at each depth. Calculation based on the formula presented in the work of Seeberg-Elverfeldt et al. (2005)

shows that pore-water extraction interval was c.a. 2.5 cm so only minor smearing of pore-water profiles can be caused during 2-cm interval sampling.

For all analyses of bulk sediment concentrations cores were sliced (slices thickness 2 cm) under an oxic atmosphere and sediment samples were analyzed or preserved for further analyses immediately. Freeze-dried sediment was used for total iron and total organic carbon analyses; fresh sediment was used for cyanide, thiocyanate, sediment roots content and roots cyanide content analyses. Hermetically closed samples stored at 4 °C were used for porosity determination.

2.2 Pore-water Composition Analysis

Total sulfide concentrations in the pore-waters were measured by spectrophotometry according to Cline (1969).

Thiosulfate concentrations in pore-water were measured by derivatization with monobromobimane, followed by HPLC separation with fluorescent detection according to Zopfi et al. (2008) with minor changes in the stationary phase and gradient program. Prevail C18 Alltech reverse phase column (250 mm × 4.6 mm × 5 μm) was used for HPLC separation of thiosulfate. Eluent A was 0.25 % (v/v) acetic acid (pH 3.5) adjusted with 5 mol L^{-1} NaOH; eluent B was 100 % HPLC-grade methanol. The following gradient conditions were used: start 10 % B, 14 min 12 % B, 30–38 min 30 % B, 54 min 42 % B, 82 min 80 % B, 84–88 min 100 % B, 90–95 min 10 % B. Mobile phase flow rate was 1 mL min^{-1}.

Thiocyanate concentrations in pore-waters were analyzed by HPLC with UV detection according to Rong et al. (2005). Thiocyanate blank concentrations were measured for all samples, which were analyzed for cyanide content, and respective concentrations of thiocyanate in the blank samples were subtracted from results of cyanide analysis.

Cyanide-reactive zero-valent sulfur in pore-waters was analyzed according to Kamyshny (2009). A sample was boiled with an excess of cyanide, and resulting thiocyanate was analyzed according to Rong et al. (2005).

Pore-water cyanide concentrations were measured according to Kamyshny et al. (2012) by derivatization with potassium tetrathionate. Reactions between cyanide and zero-valent sulfur species have been used for decades as the basis for analytical techniques for detection of the latter. In a recent publication, we applied this process to the quantification of free and metal-complexed cyanide. This method is based on a reaction of various forms of cyanide with an excess of potassium tetrathionate. Resulting thiocyanate was analyzed according to Rong et al. (2005). Free and metal-complexed cyanide (e.g., $K_4[Fe(CN)_6]$, $K_3[Fe(CN)_6]$, $K_2[Zn(CN)_4]$, $K_2[Cd(CN)_4]$, $K[Ag(CN)_2]$ and $K_2[Ni(CN)_4$) quantitatively react with tetrathionate by heating a mixture of 1 mL of pore-water with 0.1 mL of 100 mmol L^{-1} tetrathionate solution and 0.1 mL of 200 mmol L^{-1} boric acid/200 mmol L^{-1} sodium chloride solution (pH 4.4) to 90 °C for 12 h. The exceptions are $K[Au(CN)_2]$ and $K_3[Co(CN)_6]$ complexes, which cannot be detected by tetrathionate derivatization. Free cyanide and weak metal cyanide complexes (e.g., $K_2[Zn(CN)_4]$, $K_2[Cd(CN)_4]$, $K[Ag(CN)_2]$ and $K_2[Ni(CN)_4$) quantitatively react with tetrathionate by heating a mixture of 1 mL of pore-water with 0.1 mL of 100 mmol L^{-1} tetrathionate solution and 0.1 mL of 100 mmol L^{-1} boric acid/100 mmol L^{-1} sodium chloride/88 mmol L^{-1} sodium hydroxide solution (pH 10.0) to 90 °C for 20 min. Stronger cyanide complexes are not reactive toward tetrathionate in solutions with basic pH. Background concentrations of thiocyanate in the marsh pore-waters were subtracted from analyses results. Concentration of complexed cyanide was calculated as a difference between results of analysis with pH 4.4 or

pH 10.0 buffers. Although derivatization in the presence of pH 10.0 buffer accounts not only for free but for weakly complexed cyanide as well (e.g., $K_2[Zn(CN)_4]$, $K_2[Cd(CN)_4]$, $K[Ag(CN)_2]$, and $K_2[Ni(CN)_4]$), these metals are not as abundant as iron in the DGM sediments, and we assume that cyanide, which reacts with tetrathionate at pH = 10.0, is not complexed. Derivatization in the presence of pH 4.4 buffer accounts for free cyanide and all cyanide complexes except those with gold and cobalt. Since iron is the main metal which may form complexes with cyanide and thiocyanate in the marsh, we used operational definitions "free cyanide" and "complexed cyanide" in this work. It should be mentioned that although the limit of cyanide detection is 0.25 μmol L^{-1}, its concentration is calculated as a difference between thiocyanate concentrations after and before tetrathionate derivatization, and therefore, reported concentrations of cyanide sometimes are below 0.25 μmol L^{-1}, or even negative. Standard deviation of analysis of concentrations of free and complexed cyanide is 10 % (Kamyshny et al. 2012).

Soluble Fe(II) in the pore-waters was analyzed by spectrophotometry using AQUANAL®-plus iron (Fe) 0.02–0.2 mg/L kit.

2.3 Sediment Composition Analysis

Porosity and sediment density were measured by addition of water to pre-weighted sediment of the total volume of 10 mL, drying for a week at 50 °C and measuring of the weight of dried sediment. Sediments of the DGM contain large amount of roots and thus are highly non-homogenous. Results of above measurements in certain depth intervals were averaged. The following average values for porosity measurements were obtained for October 30, 2009 sampling: 0.83 at <6 cm depth, 0.72 at 6–24 cm depth, and 0.62 at >24 cm depth. For April 14, 2010 sampling, average porosity values were 0.77 at <6 cm depth, 0.73 at 6–24 cm depth, and 0.65 at >24 cm depth. Average wet sediment density was 1.1 kg l^{-1}.

Roots content of the bulk sediment was measured by shaking of weighted sediment with Milli-Q water, followed by manual separation of roots, drying roots with paper towels and weighing roots. A following average values for sediment root content were obtained for October 30, 2009 sampling: 20 % at <6 cm depth, 31 % at 6–18 cm depth, and 11 % at >18 cm depth. For April 14, 2010 sampling, average porosity values were 15 % at <6 cm depth, 35 % at 6–18 cm depth, and 14 % at >18 cm depth.

A fraction of sediment, which visually had relatively low root content, was used for analysis of cyanide and thiocyanate content of the wet sediment. For cyanide determination, 0.5–1.5 g of sediment was mixed with 9 mL Milli-Q water, 1 mL pH = 4.4 buffer (Kamyshny et al. 2012) and 0.2 mL 500 mmol L^{-1} of potassium tetrathionate solution, shaken for 15 min and heated overnight at 90 °C. The sample was centrifuged, and the supernatant was analyzed for thiocyanate concentration according to Rong et al. (2005). For thiocyanate determination, 10 mL of pH = 4.4 (Kamyshny et al. 2012) buffer was added to 1.6–4.6 g of sediment and the sample was shaken overnight. Thiocyanate concentration in supernatant was detected after centrifugation according to Rong et al. (2005).

Free cyanide content of *Spartina alterniflora* grass roots was detected during the October 30, 2009 sampling for the fraction of roots at 10–20 cm depth. Roots (10 g) were pulverized with 190 mL of Milli-Q water, shaken for 15 min and centrifuged. Hydrogen cyanide content in the supernatant was measured by tetrathionate derivatization with pH = 10.0 buffer. The concentration of thiocyanate formed during the derivatization was measured according to Rong et al. (2005).

Total iron analysis was performed according to Aller et al. (1986) by heating of freeze-dried sediment in the muffle oven for 8 h at 450°C, followed by heating for 24 h with concentrated hydrochloric acid. Hydrochloric acid extract was diluted 100 times and analyzed for iron content by atomic absorbance spectrometry with iCE 3000 Series Thermo Finnigan AAS.

The total inorganic carbon content was measured by CO_2 Coulometer CM 5012 with an Acidification Module CM 5130, and the total carbon content was measured by CNS elemental analyzer NA 1500 NC (Fisons Instruments). Total organic carbon content of freeze-dried sediment was calculated as a difference between the total carbon and total inorganic carbon.

2.4 Slurry Preparation and Incubation

A core for slurry incubations was sectioned under anoxic atmosphere (typically < 0.2 % O_2) in the glove bag. Slurry for incubation experiments was prepared by mixing of c.a. 785 mL of sediment, collected from the core retrieved on April 14, 2010 sampling with 785 mL of artificial deoxygenated seawater (main constituents only, no nutrients were added) with pH adjusted to 8.0 in the glove box under anoxic conditions. The slurry was homogenized and divided in three equal portions. Each portion was transferred to a zip-lock plastic bag and spiked with thiocyanate, polysulfide or cyanide by adding small volume (<1 mL) of concentrated stock solution. Concentrations of spiking species were such as to allow easy quantification by HPLC analysis (60–1,200 μmol L^{-1}). Sub-samples for time series experiments were taken by transferring a portion of the slurry into 50-mL falcon tube in the glove box. Analyses were performed in the similar way as for sediment samples.

2.5 Definitions of Cyanide and Thiocyanate Pools in Sediment

Free hydrogen cyanide pore-water concentration (CN_{free}) (measured)

Strongly (iron) complexed cyanide pore-water concentration (CN_{Fe}) (measured)

Pore-water cyanide (CN_{pw}), calculated as $CN_{pw} = CN_{free} + CN_{Fe}$

Wet sediment cyanide (CN_{sed}) (measured)

Adsorbed cyanide (CN_{ads}), calculated as $CN_{ads} = CN_{sed} - CN_{pw}$

Sedimentary content of free hydrogen cyanide in the roots of *Spartina alterniflora* grass (CN_{roots}), calculated as CN_{roots} = [HCN in roots] × Weight fraction of roots in sediment, where

[HCN in roots] = 50.0 μmol kg^{-1}

Pore-water thiocyanate (SCN_{pw}) (measured)

Wet sediment thiocyanate (SCN_{sed}) (measured)

Adsorbed thiocyanate (SCN_{ads}), calculated as $SCN_{ads} = SCN_{sed} - SCN_{pw}$

Total cyanide pool CN_{total}, calculated as $CN_{total} = CN_{pw} + CN_{sed} + CN_{roots} + SCN_{pw} + SCN_{sed}$

Pore-water concentrations of cyanide and thiocyanate species are presented in μmol L^{-1} and concentrations in the wet sediment in μmol kg^{-1}.

For estimation of fractions of dissolved cyanide and thiocyanate pools in the total cyanide pool, concentrations of dissolved pools in total sediment were calculated as

$[(S)CN]_{sediment}$, μmol $kg^{-1} = [(S)CN]_{pore\text{-}water}$, μmol $L^{-1} \times \varphi \times \rho^{-1}$, where

φ is porosity, and ρ is sediment density in kg L^{-1}.

3 Results

3.1 Sedimentary Profiles

In October, free cyanide concentrations in pore-waters of DGM were in the range of 0.06–0.49 μmol L^{-1}. The highest concentrations of free cyanide were detected at 3–19 cm depth (Fig. 1a). In April, the concentrations of free cyanide were much higher at 3 and 31 cm depths (1.11 and 1.92 μmol L^{-1}, respectively). At 11–19 cm depths, cyanide was not detected (Fig. 1a). Concentrations of cyanide strongly complexed with metal, in pore-waters of DGM in October, were found to be <1 μmol L^{-1} at all depths except 15 × 19 cm, where 2.25–6.94 μmol L^{-1} of metal-complexed cyanide was detected (Fig. 1a). In April, concentrations of strongly metal-complexed cyanide were detected at 7–11 cm depth (2.70–5.71 μmol L^{-1}) (Fig. 1a).

Cyanide concentrations in wet sediment in October were found to be as high as 230 μmol kg^{-1} (6 ppm CN^-) near the sediment surface. Sediment cyanide content steadily decreased to 29 μmol kg^{-1} at 11 cm depth and was 5–45 μmol kg^{-1} below this depth (Fig. 1b). In April, the highest sediment cyanide content was measured at 7 cm depth (65 μmol kg^{-1}). At 3 cm depth, it was only 2.7 μmol kg^{-1}, and below 7 cm depth, it was in the 15–50 μmol kg^{-1} range (Fig. 1b).

The cyanide content of wet root from the 10–20-cm depth interval was found to be 50.0 μmol kg^{-1} during the April sampling.

The highest pore-water thiocyanate concentration in pore-waters in October was detected at 19 cm depth (1.78 μmol L^{-1}). Concentrations of thiocyanate decreased toward sediment surface (0.43 μmol L^{-1} at 1 cm) and toward deep sediment (1.18 μmol L^{-1} at 35 cm depth) (Fig. 1c). In April, 2.28 μmol L^{-1} was detected at 25 cm depth. Concentrations of thiocyanate decreased at shallower depths to 1.01 μmol L^{-1} at 7 cm depth with higher value of 1.46 μmol L^{-1} in the surface sediment (Fig. 1c).

The highest thiocyanate content of wet sediment was detected in the surface sediments in October (15.6 μmol kg^{-1}). It decreased with depth to 1.8 μmol kg^{-1} at 11 cm depth and stayed in the range 0.8–1.8 μmol kg^{-1} below this depth. In April, the highest sediment thiocyanate content was detected at 3 cm depth and 29 cm depth (4.68 and 4.65 μmol kg^{-1}, respectively). Between these depths, it was in the 1.5–2.4 μmol kg^{-1} range.

In October, sulfide in pore-waters was detectable in surface sediments (0.86 mmol L^{-1}). It increased with depth to 6.05 mmol L^{-1} at 19 cm depth. Below this depth, sulfide concentration decreased with depth to 3.49 mmol L^{-1} at 35 cm (Fig. 1e). In April, surface sediments contained no free sulfide. Sulfide in pore-waters was detectable at ≥ 13 cm depth with the highest concentration 5.41 mmol L^{-1} at 25 cm depth (Fig. 1e).

The highest concentration of cyanide-reactive zero-valent sulfur in pore-waters in October, 56 μmol L^{-1}, was detected at 7 cm depth. In the surface sediment, it was only 14 μmol L^{-1}, and at 19–35 cm depth, it was in the range of 13–16 μmol L^{-1} (Fig. 1f). Profile of thiosulfate concentrations was similar to the profile of cyanide-reactive zero-valent sulfur with maximum of 50 μmol L^{-1} at 7 cm depth and 12–35 μmol L^{-1} at other depths (Fig. 1f). In April, concentrations of both cyanide-reactive zero-valent sulfur and thiosulfate were found to be low (≤7 μmol L^{-1}) in the upper, non-sulfidic, sediment layer (Fig. 1f). The highest cyanide-reactive zero-valent sulfur concentrations were detected at 19–29 cm depth (43–78 μmol L^{-1}), and the highest thiosulfate concentrations were detected at 15–21 cm depths (91–114 μmol L^{-1}) (Fig. 1f).

Fig. 1 **a** Profiles of pore-water hydrogen cyanide concentration. *Black circles* represent free and weakly ▶ metal-complexed cyanide—October 30, 2009 sampling, *black rectangles* represent strongly metal-complexed cyanide—October 30, 2009 sampling, *blue diamonds* represent free and weakly metal-complexed cyanide—April 14, 2010 sampling, and *blue triangles* represent strongly metal-complexed cyanide—April 14, 2010 sampling. **b** Profiles of cyanide content in wet sediment. *Black circles* represent October 30, 2009 sampling, and *blue diamonds* represent April 14, 2010 sampling. **c** Profiles of pore-water thiocyanate concentration. *Black circles* represent October 30, 2009 sampling, and *blue diamonds* represent April 14, 2010 sampling. **d** Profiles of thiocyanate content in wet sediment. *Black circles* represent October 30, 2009 sampling, and *blue diamonds* represent April 14, 2010 sampling. **e** Profiles of total sulfide concentration in pore-water. *Black circles* represent October 30, 2009 sampling, and *blue diamonds* represent April 14, 2010 sampling. **f** Profiles of pore-water cyanide-reactive S^0 and thiosulfate concentrations. *Black circles* represent cyanide-reactive S^0—October 30, 2009 sampling, *black rectangles* represent thiosulfate—October 30, 2009 sampling, *blue diamonds* represent cyanide-reactive S^0—April 14, 2010 sampling, and *blue triangles* represent thiosulfate—April 14, 2010 sampling. **g** Profiles of pore-water Fe(II) concentration. *Black circles* represent October 30, 2009 sampling, and *blue diamonds* represent April 14, 2010 sampling. **h** Profiles of total iron content in dry sediment. *Black circles* represent October 30, 2009 sampling, and *blue diamonds* represent April 14, 2010 sampling. **i** Profiles of total organic carbon content in dry sediment. *Black circles* represent October 30, 2009 sampling, and *blue diamonds* represent April 14, 2010 sampling. Pore-waters were extracted with Rhizon samplers at 2-cm interval, and core for bulk sediment analysis was sliced in 2-cm intervals. Each depth value in both pore-water and bulk sediment concentration profiles has ±1-cm interval. *Red line* depicts depth of iron-sulfide transition zone during April 14, 2010 sampling

In October, concentrations of iron in pore-water was <0.6 μmol L^{-1} at all depths. In April, in the upper, non-sulfidic sediment layer, 1.4–6.3 μmol L^{-1} of iron was detected (Fig. 1g).

In October, total dry sediment iron content of sediment was 495–729 mmol kg^{-1} with the highest concentration detected near the surface. In April, total sedimentary iron content was 430–882 mmol kg^{-1} with the highest concentration detected near the surface and at 25 cm depth (Fig. 1h).

Dry sediment TOC concentration profiles in both October and April generally decreased with depth and were in the range 3.5–8.4 mol kg^{-1} (Fig. 1i).

3.2 Incubations

We conducted incubations of sediment slurries to gain a better understanding of the fate of cyanide, zero-valent sulfur and thiocyanate in the salt marsh sediments. Slurries were prepared from sediment retrieved on April 14, 2010. Sediment from a depth interval of 10–20 cm depth, which roughly corresponds to the upper part of sulfide-rich zone, was spiked with (a) thiocyanate, (b) cyanide and (c) polysulfide. We measured concentrations of thiocyanate, cyanide and cyanide-reactive zero-valent sulfur in the aqueous phase as well as concentrations of cyanide and thiocyanate in the slurry as a function of time (Fig. 2).

Thiocyanate concentration showed no change in the aqueous phase (Fig. 2a) and in the whole sediment over a period of 64 h.

Polysulfidic zero-valent sulfur added to sediment disappeared very rapidly (>50 % in the first hour) (Fig. 2b). In the first 7 min after spiking pore-water, thiocyanate concentration increased by 3.29 μmol L^{-1}, which accounts for 40 % of total (mostly iron-complexed) cyanide in the pore-water.

When cyanide was added to the slurry, conversion to thiocyanate occurred in hours (48 and 62 % in 22 and 64 h, respectively) (Fig. 2c). While the concentration of free cyanide decreased with time, the concentration of complexed cyanide slowly increased, reaching 11.8 % of total added cyanide after 64 h of incubation. Adsorbed cyanide fraction decreased during the first hour of slurry incubation (Fig. 2d). Adsorbed thiocyanate was not detected in the course of incubation.

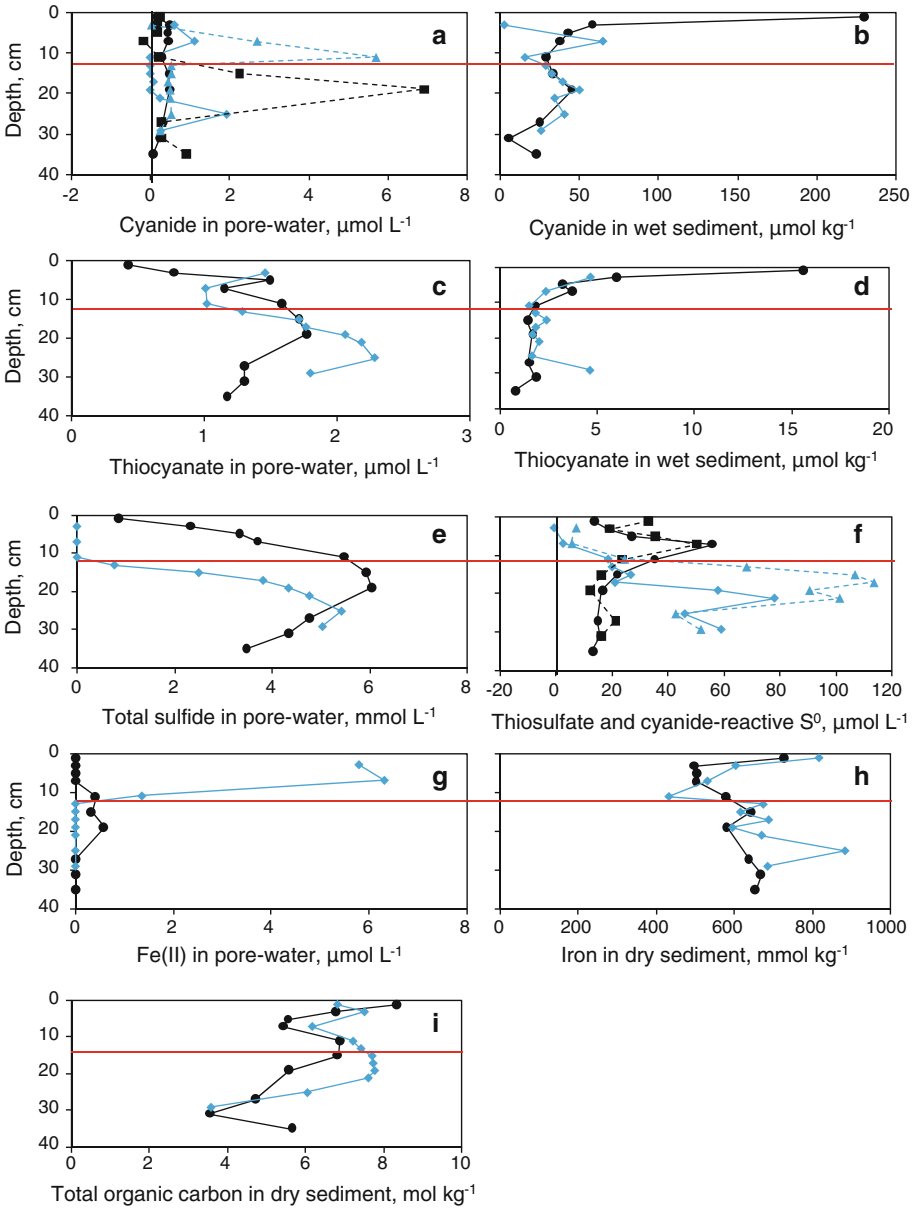

4 Discussion

4.1 Delaware Great Marsh sediments

We propose that one of the sources of hydrogen cyanide in marsh sediments is associated with decomposition of *Spartina alterniflora* roots, which were found to contain 50.0 µmol kg^{-1} cyanide during the April sampling. This is supported by the observation

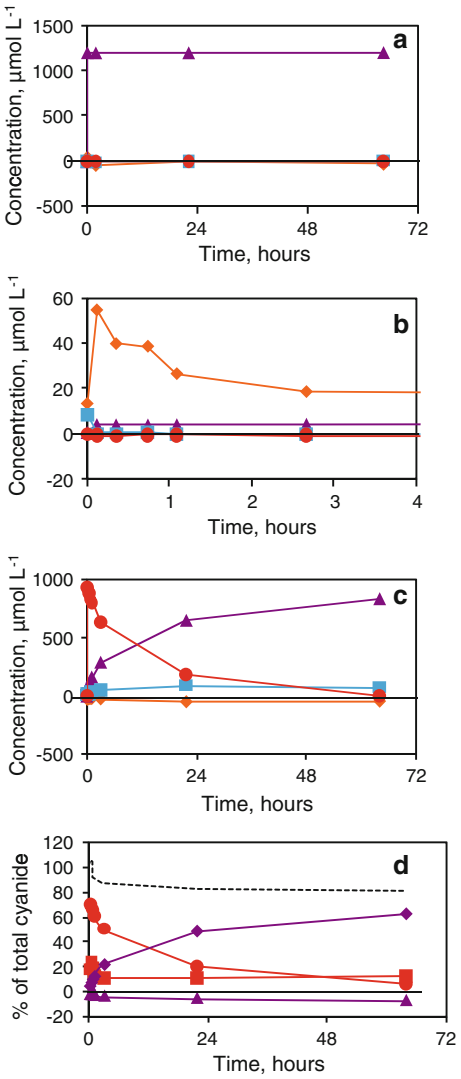

Fig. 2 Time series profiles of concentrations of free cyanide (*red circles*), complexed cyanide (*blue rectangles*), cyanide-reactive S^0 (*orange diamonds*) and thiocyanate (*violet triangles*) in the experiments of sediment amendment with thiocyanate (**a**), polysulfides (**b**) and cyanide (**c**). (**d**) represents fractions of dissolved cyanide (*red circles*), adsorbed cyanide (*red rectangles*), dissolved thiocyanate (*purple diamonds*) and adsorbed thiocyanate (purple triangles) in the experiments of sediment amendment with cyanide. *Black dashed* line represents recovery of all species included in the total cyanide pool. All recoveries are normalized to the total cyanide pool after 2 min of incubation. Negative concentrations result from subtraction of thiocyanate content in pore-waters from thiocyanate content of slurry (see text for details). Zero-time point reflects concentrations of relevant species in non-amended sediment slurry

that sedimentary cyanide content in October, when fast decomposition of organic matter occurs, is higher than in April (Fig. 1b). There may exist cyanide sources other than *Spartina alterniflora* roots in the DGM sediments: cyanide is known to be produced by a variety of plants, fungi, algae and bacteria (Wong-Chong et al. 2006b). It is possible as well that decomposing root of *Spartina* provide carbon and nitrogen species, which are converted to cyanide by microorganisms. As no support for cyanogenesis by *Spartina* was found in the literature, further research on cyanide sources in the marsh sediments is needed to resolve the ultimate source of the cyanide.

In the following discussion, we focus on iron-cyanide complexes because other cyanide-complexing metals (e.g., Zn, Cu, Mn, Ni) in the marsh are at lower abundance than iron and because cyanide complexes of these metals are much weaker than the ferrocyanide complex.

Hydrogen cyanide, which is released into anoxic and dark salt marsh sediments, may stay in pore-water as free hydrogen cyanide or undergo various transformations. In Fe(II) rich waters above the sulfidic layer, cyanide can form a strong ferrocyanide complex, $[Fe(CN)_6]^{4-}$. A concentration of pore-water Fe(II) of >1 μmol L^{-1} was detected only above the sulfide-rich zone (Fig. 1g). The equilibrium constant $K = 7.1 \times 10^{36}$ for:

$$Fe^{2+} + 6\ CN^- \rightleftarrows Fe(CN)_6^{4-} \quad (1)$$

was proposed by Keefe and Miller (1996) for ferrocyanide formation in the seawater at 25 °C, and it can be used to show that at 1 μmol L^{-1} concentration of free cyanide and free iron(II), the ratio of iron(II)-complexed cyanide to free cyanide concentrations is 42.6. pK_a of HCN at infinite dilution is 9.21, and dissociation of iron-cyanide complexes occurs at acidic conditions (Eq. 2).

$$Fe(CN)_6^{4-} + 6\ H^+ \rightleftarrows Fe^{2+} + 6\ HCN \quad (2)$$

In October, pH of pore-waters was in the range 7.0–7.6 for all sediment depths. In April, pH of pore-waters was in the 6.5–7.7 range, at all depths except 3-cm sample (pH = 3.73). At near neutral and acidic conditions, virtually all cyanide, which is dissolved in pore-waters, should exist in a free rather than in iron-complexed form. Thus, kinetic rather thermodynamic factors should control cyanide speciation in the pore-waters. In the dark at pH 4, estimates of the half-life of ferrocyanide range from 1 year under reducing conditions to 1,000 years under oxidizing conditions (Meeussen et al. 1992). Dissociation of iron-cyanide complexes is known to be accelerated by light (Meeussen et al. 1992; Dzombak et al. 2006b, and references therein).

Cyanide can also be adsorbed on iron (III) oxide minerals, clays and sedimentary organic matter (Chatwin et al. 1988). Iron-cyanide complexes have been shown adsorb on aluminum and iron(III) oxides, especially at acidic pH (Dzombak et al. 2006b and references therein). HCN adsorbs on inorganic phases more weakly than CN^-. Within the pH range 4–9, organic carbon should be the most important sediment constituent for hydrogen cyanide adsorption (Dzombak et al. 2006b).

The total iron content of the sediment was between 430 and 815 mmol kg^{-1} of dry sediment (Fig. 1h). Local maxima of total iron concentrations were detected in the upper 2–4 cm of sediment during both samplings. These results are in agreement with the results reported by Kostka and Luther (1994, 1995), who measured total iron concentrations in the range of 200–600 mmol kg^{-1} in the dry sediment on the same site, with the higher total iron concentrations near the sediment surface in the vegetated site (Kostka and Luther 1995). Pyrite iron content was generally an order of magnitude lower than the total iron content (data not shown, pyrite content was analyzed by chromium reducible sulfur distillation). Although adsorption of cyanide on iron phases is less important than adsorption on organic matter, iron(III) hydroxide reactions with cyanide produce sulfide oxidation intermediates, which are reactive toward cyanide (see detailed discussion below). Iron(III) (hydr)oxides (except magnetite) are reduced by hydrogen sulfide on a minutes to months timescale (Canfield 1989; Canfield et al. 1992) and thus should also not comprise the main iron fraction. On the other hand, silicate-associated iron oxides are known to react with sulfide on a timescale of hundreds to hundreds of thousands years (Canfield et al. 1992). Thus, we propose the total iron is mostly represented by silicate-associated Fe(III) oxides.

The total organic carbon (TOC) content of the sediment was 3.5–8.4 mol kg^{-1} dry sediment and generally decreases with depth (Fig. 1i). The highest TOC content was detected in the upper two centimeters of sediment during the October 30, 2009 sampling,

coinciding with the highest content of cyanide (230 μmol kg^{-1}, 6 ppm in the wet sediment) (Fig. 1b). During this period of the year, the whole sediment column was found to be sulfide rich (Fig. 1e).

Another possible cyanide sink in the marsh sediments is provided by conversion of cyanide complexes to thiocyanate, by reaction with sulfide oxidation intermediates. Sulfide oxidation intermediates, which have sulfur–sulfur bonds, are known to be reactive toward free cyanide (Kelly et al. 1969; Szekeres 1974; Luthy and Bruce 1979; Kamyshny 2009; Kamyshny et al. 2009). Polysulfides, polythionates with four or more sulfur atoms, and soluble and colloidal elemental sulfur react with cyanide faster than trithionate and thiosulfate (Kelly et al. 1969; Luthy and Bruce 1979; Kamyshny et al. 2009). Polysulfides are known to react rapidly with hydrogen cyanide via:

$$S_n^{2-} + (n-1)\mathrm{HCN} \rightarrow \mathrm{HS}^- + (n-1)\mathrm{SCN}^- + (n-2)\mathrm{H}^+, \quad \text{where } n = 2-8 \tag{3}$$

This reaction is irreversible: for the reaction of pentasulfide ion with hydrogen cyanide, ΔG_r^0 is −36.8 kJ mol^{-1} per thiocyanate anion formed. The reaction of $[Fe(CN)_6]^{4-}$ with pentasulfide is even more energetically favorable, and the ΔG_r^0 is −57.2 kJ mol^{-1} per thiocyanate anion formed (Eq. 4).

$$3\ S_5^{2-} + 2\left[\mathrm{Fe(CN)_6}\right]^{4-} + 3\mathrm{H}^+ \rightarrow 3\ \mathrm{HS}^- + 12\ \mathrm{SCN}^- + 2\ \mathrm{Fe}^{2+} \tag{4}$$

At concentrations typical for the DGM ([HCN] = 1 μmol L^{-1}, [polysulfide-S^0] = 100 μmol L^{-1}, pH = 8.2, T = 25 ± 1 °C), 19 nmol L^{-1} h^{-1} of cyanide will be converted to thiocyanate by reaction (3) as calculated using the rate equation from Luthy and Bruce (1979). Transfer of sulfur atoms from sulfur donors to cyanide is catalyzed by rhodanese, an enzyme that detoxifies cyanide, which is found in a variety of microorganisms and in mammalian tissues (Knowles 1976). Sulfide oxidation intermediates are formed by oxidation of sulfide, especially with mild oxidation agents such as Fe(III) (hydr)oxides (Yao and Millero 1996) and MnO_2 (Yao and Millero 1993). Polysulfides may be also formed by reaction of sulfide with solid sulfur (Boulegue and Michard 1977):

$$\mathrm{HS}^- + (n-1)/8\ \mathrm{S_8} \rightleftarrows \mathrm{H}^+ + \ S_n^{2-} \tag{5}$$

Tetrathionate has been shown to be reactive toward iron-complexed cyanide as well at pH = 4.4 and elevated temperatures (Kamyshny et al. 2012).

Profiles of cyanide, thiocyanate and reactive sulfur species further testify to formation of thiocyanate by this pathway. Biogeochemical processes in the marsh sediments depend on the redox potential of the system, which is why we use the depth of the iron-sulfide transition zone as a reference for our depth scale. In October, sulfide was detected in the surface sediment (Fig. 1e), and thus, the depths of iron-sulfide transition zone will be assumed to be 0 cm. In April, sulfide was detectable at 13 cm depth and non-detectable at 11 cm depth, and thus, the iron-sulfide transition zone depth will be assumed to be 12 cm.

In October, the maximum concentrations of free cyanide and strongly complexed cyanide were detected to be 3–19 cm and 15–19 cm below iron-sulfide transition zone, respectively (Fig. 1a). Overall concentrations of free cyanide in October were relatively low, and the highest concentrations were only twice as high as the detection limit of analysis. At the same depth interval, 5–19 cm, the highest concentrations of thiocyanate were detected in the pore-waters (Fig. 1c). The highest concentrations of both adsorbed cyanide and thiocyanate were detected in the surface sediment (Figs. 1b, d). Cyanide-reactive zero-valent sulfur concentrations above 20 μmol L^{-1} were detected as well at 5–15 cm depth (Fig. 1f). At 5–11 cm depth, the concentrations of thiosulfate are as well

above 20 μmol L^{-1}. In the surface sediment layer, where concentrations of reactive sulfur species are lower, accumulation of cyanide in the sediment occurs.

In April, free cyanide was detected at 5–9 cm above iron-sulfide transition zone and at 15–23 cm below iron-sulfide transition zone (Fig. 1a). The highest concentrations of strongly complexed cyanide were detected in the iron-rich layer (7–9 above iron-sulfide transition zone), although strongly complexed cyanide was detectable at all depths. Adsorbed cyanide showed a profile similar to that of free cyanide: with a high concentration at −5 cm relative to iron-sulfide transition zone, with a sharp decrease at iron-sulfide transition zone and with relatively high concentrations 4–13 cm below iron-sulfide transition zone (e.g., at lower depths than free cyanide) (Fig. 1b). Free thiocyanate concentrations are not significant at iron-sulfide transition zone with a sharp increase immediately below it and a maximum at 13 cm depth relative to iron-sulfide transition zone (Fig. 1c). The concentration of adsorbed thiocyanate is relatively low at, and below, the iron-sulfide transition zone (Fig. 1d).

We propose that the coincidence of high concentrations of cyanide, reactive sulfur species and thiocyanate in the marsh sediments in October is due to chemical thiocyanate production by a reaction between cyanide species and reactive sulfur (especially zero-valent) species. High rates of decomposition of organic matter in the marsh result in a cyanide flux high enough to maintain detectable cyanide concentrations even in the presence of reactive sulfur species. In April, the cyanide production is slower and in the vicinity of iron-sulfide transition zone, where concentrations of cyanide-reactive zero-valent sulfur are high, cyanide, which is released into the marsh, reacts with cyanide-reactive zero-valent sulfur immediately. Even the content of adsorbed cyanide sediment decreases at the iron-sulfide transition zone due to the reaction with reactive sulfur intermediates.

Other possible cyanide sinks include oxidation to cyanate, which occurs under oxic conditions, biodegradation and volatilization (Chatwin et al. 1988). Biodegradation of cyanide under oxic conditions has been well studied (Wild et al. 1994). Bacterial consumption of cyanide in anaerobic bacterial cultures and during wastewater treatment has also been documented (Wild et al. 1994).

In marsh sediments, the main constituents of the CN_{total} were adsorbed cyanide and cyanide in the *Spartina alterniflora* roots (Fig. 3). Strongly complexed cyanide and free cyanide fractions of the total cyanide were <17 and <4 %, respectively. Adsorbed thiocyanate prevailed over dissolved thiocyanate usually in the shallow sediment, possibly due to adsorption on sedimentary organic matter. A relatively large amount of free thiocyanate was found below 10 cm absolute depth.

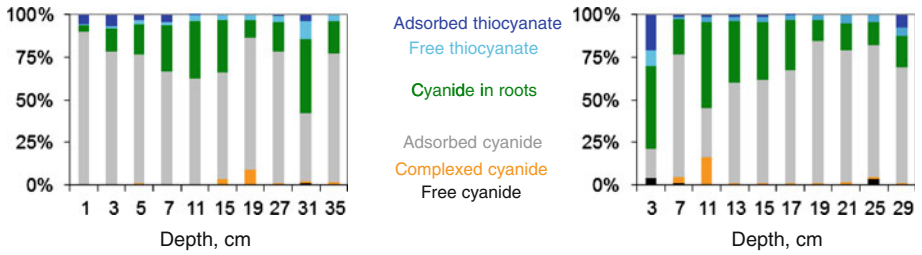

Fig. 3 Relative abundance of various components of total cyanide species during the October 30, 2009 sampling (*left panel*) and April 14, 2010 sampling (*right panel*). Each depth value reported has ±1-cm interval as pore-waters, and solid phase were sampled with 2-cm intervals

4.2 Sediment Amendment Incubations

Variation in dissolved thiocyanate concentration during 64 h of incubation was below 0.2 % (Fig. 2a). This observation suggests that in anoxic sulfide-rich sediment thiocyanate is stable and is not consumed by abiotic or biologically assisted processes on the scale of days. There are other independent confirmations to this observation. First, the shapes of profiles of thiocyanate concentrations in pore-water (Fig. 1c) and in sediment (Fig. 1d) are evidence of strong thiocyanate adsorption on sediment in the upper sediment layer and also its degradation in the upper layer, and possibly throughout the oxic sediment zone. Second, the stability of thiocyanate under anoxic conditions is in accordance with observations that in stratified water columns of two lakes, thiocyanate concentrations decrease from the bottom to the redox-transition zone, and thiocyanate disappears with the onset of oxygen (Kamyshny et al. 2011). However, it should be mentioned that in these lakes, a thiocyanate offset occurs in the water layer populated by purple sulfur bacteria, which possibly metabolize thiocyanate. On the other hand, thiocyanate was detected as well in non-stratified oxic water bodies, such as North Sea water (13 nmol L^{-1}, Kamyshny 2009), waters of Japanese ports (140–259 nmol L^{-1}, Rong et al. 2005) and waters near the Tuas industrial zone in Singapore (60 ± 18 nmol L^{-1}, Kamyshny and Lev, unpublished data).

Bacterial thiocyanate degradation has been extensively studied in industrial activated sludge reactors for treatment of wastewaters and especially industrial coke wastewaters. It has been shown that in anaerobic reactors, bacterial degradation of thiocyanate is either slow or does not occur (Shieh and Richards 1988; Chakraborty and Veeramani 2006; Kim et al. 2008; Sahariah and Saswati 2011). These results are consistent with the results of our incubation experiments. On the other hand, the same studies showed that under oxic conditions, thiocyanate is rapidly degraded. Shieh and Richards (1988) even showed that the same microbial community, which does not degrade thiocyanate under anoxic conditions, may restore its thiocyanate degrading capability immediately after a return to oxic conditions. It was also shown that the presence of thiosulfate and cyanide inhibits microbial uptake of thiocyanate (Karavaiko et al. 2000). The main products of bacterial thiocyanate degradation under oxic conditions were shown to be ammonia and carbonyl sulfide (which undergoes subsequent hydrolysis to hydrogen sulfide and carbon dioxide) or hydrogen sulfide and cyanate (which is subsequently hydrolyzed to ammonia and carbon dioxide) (Stratford et al. 1994; Wood et al. 1998) Interestingly, thiocyanate may be degraded as well to tetrathionate (Stratford et al. 1994), which in turn is reactive toward cyanide and its complexed forms (Kamyshny 2012).

Zero-valent sulfur added in the form of soluble polysulfides disappears in the marsh sediment pore-waters in hours, mostly by processes other than reaction with cyanide. In the first seven minutes, 3.29 μmol L^{-1} of thiocyanate is produced, followed by slow increase by 1.21 μmol L^{-1} in the next 63 h. We attribute the initial rapid increase in thiocyanate concentrations to reaction between polysulfides in high concentrations and free cyanide. The ensuing slow increase in thiocyanate concentrations may be attributed to the reaction between polysulfides in small amounts of cyanide released due to decomposition of sedimentary organic matter in course of incubation (Fig. 2b).

When added to sediment slurries, free cyanide shows a steady decrease in concentration in pore-waters. Most of the cyanide is converted to pore-water thiocyanate. A small proportion of the cyanide immediately adsorbs onto the sediment solid phase and then slowly reacts with sedimentary reactive sulfur species. After 3 h, the fraction of cyanide in the adsorbed form is stabilized and slowly increases from 10.3 to 11.8 % between 3 and 64 h of incubation. We attribute this behavior to a fast reaction of both free and adsorbed

cyanide with highly reactive zero-valent sulfur compounds (e.g., polysulfides) during the first hour of incubation, followed by a slow cyanide reaction with thiosulfate and polysulfides, which are continuously formed by reaction of sulfide with sedimentary solid sulfur (Eq. 5). Thiosulfate and polysulfides are present in the sediment at concentrations of 7–72 mmol kg^{-1} in the 10–20-cm depth interval (Fig. 2c).

CN_{total} (roots were analyzed as part of solid phase) decreases to 81–82 % of the initial value after 1–3 days of incubation which we explain as being due to degassing of hydrogen cyanide during sampling of the slurry from bags. Conversion of 62 % of cyanide (77 % taking into account HCN degassing) to thiocyanate suggests that anaerobic microbial degradation of cyanide (to species other than thiocyanate) is not a quantitatively important process in these salt marsh sediments (Fig. 2d).

4.3 Conceptual Model of Cyanide and Thiocyanate Transformations

We have not attempted to build a quantitative model of cyanide and thiocyanate formation, transport and consumption due to two main reasons: (1) the Delaware Great Marsh sediments are extremely non-homogeneous, contain high and variable root content and are prone to significant bioturbation and (2) there is not enough data on kinetics of reactions between various reactive sulfur species and various cyanide species. We instead propose the following working model of cyanide production and transformations in anoxic salt marsh sediments on the basis of concentration profiles and incubation experiments (Fig. 4). Hydrogen cyanide is produced by *Spartina alterniflora* roots (and possibly other organisms) and released into the marsh sediments during processes associated with decomposition of the roots. The main fraction of hydrogen cyanide is adsorbed on the sediment, mostly on Fe(III) and organic matter rich phases. Minor fractions of cyanide remain dissolved in the pore-water either as free hydrogen cyanide or as complexed with iron. Sulfide, which is produced by bacterial sulfate reduction, is oxidized by Fe(III) (hydr)oxides to form sulfide oxidation intermediates, which are reactive toward hydrogen cyanide (e.g., thiosulfate and especially polysulfides). Free hydrogen cyanide reacts rapidly with sulfide oxidation intermediates resulting in the formation of thiocyanate. Ferrocyanide, which is formed by the reaction of free cyanide with dissolved Fe(II), either reacts slowly with sulfide oxidation intermediates or slowly decomposes to hydrogen cyanide, when pH, cyanide concentration or dissolved iron concentration decrease. Adsorption of free and iron-complexed cyanide on the sedimentary organic matter and on Fe(III) hydroxides is a temporary cyanide sink. Desorption of hydrogen cyanide and reaction of adsorbed cyanide with sulfide oxidation intermediates result as well in formation of thiocyanate. Thiocyanate formation represents the ultimate cyanide sink. Thiocyanate is stable under anoxic conditions, but much less retained on the sediment and thus diffuses to an upper oxic sediment

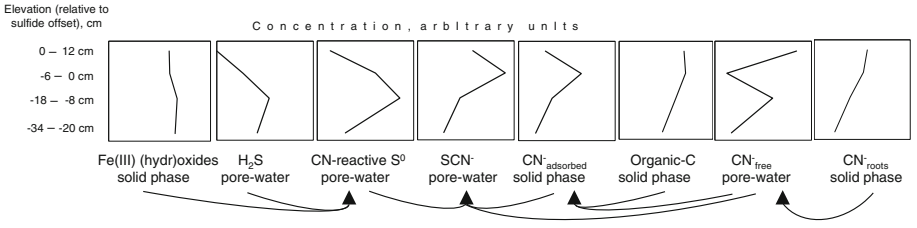

Fig. 4 Conceptual scheme of cyanide cycling in the DGM sediment and averaged profiles of relevant species

layer, where it may be oxidized by biologically assisted processes either to carbonyl sulfide and ammonia or to cyanate and hydrogen sulfide.

Acknowledgments This work was supported by the Max Planck Society (T.G.F. and A.K.), Marie Curie Outgoing International Fellowship SULFUTOPES number POIF-GA-2008-219586 (to A.K.), NSF Geobiology and Low Temperature Geochemistry Program grant number: 0843814 (to A. K., JF and Z.F.M.) and the NASA Astrobiology Institute (J.F.). The authors would like to thank George W. Luther and Andrew Madison (University of Delaware) for assistance during sampling of Delaware Great Marsh. The authors are grateful to Donald E. Canfield and Daniel L. Eldridge for valuable comments on the manuscript. The revised manuscript benefited by the comments of two anonymous reviewers and the Associated Editor David J. Burdige.

References

Aller RC, Mackin JE, Cox RT Jr (1986) Diagenesis of Fe and S in Amazon inner shelf muds: apparent dominance of Fe reduction and implications of the genesis of ironstones. Cont Shelf Res 6:263–289

Boulegue J, Michard G (1977) Dissolution du soufre elementaire dans les solutions aqueuses diluees d'hydrogene sulfure. Comptes Rendus Acad Sci Paris 284C:713–716

Canfield DE (1989) Reactive iron in marine sediments. Geochim Cosmochim Acta 53:619–632

Canfield DE, Raiswell R, Bottrell S (1992) The reactivity of sedimentary iron minerals toward sulfide. Am J Sci 292:659–683

Chakraborty S, Veeramani H (2006) Effect of HRT and recycle ratio on removal of cyanide, phenol, thiocyanate and ammonia in an anaerobic-anoxic-aerobic continuous system. Process Biochem 41:96–105

Chatwin TD, Zhang J, Gridley GM (1988) Natural mechanisms in soil to mitigate cyanide release. In: Proceedings of superfund '88, the 9th National Conference, Hazardous Materials Control Research Institute, Washington, pp 467–473

Cline JD (1969) Spectrophotometric determination of hydrogen sulfide in natural waters. Limnol Oceanogr 14:454–458

Davy AJ, Bishop GF (1991) *Triglochin maritime* (L.). J Ecol 79:531–555

Dzombak DA, Roy SB, Anderson TL, Kavanaugh MC, Deeb RA (2006a) in *Cyanide in Water and Soil*, eds Dzombak DA. Wong-Chong GM (CRC Press, Boca Raton, Florida), Ghosh RS, pp 209–224

Dzombak DA, Ghosh RS, Young TC (2006b) In: Dzombak DA, Ghosh RS, Wong-Chong GM (eds) Cyanide in water and soil. CRC Press, Boca Raton, pp 57–92

Ettlinger M, Eyjólfsson R (1972) Revision of the structure of the cyanogenic glucoside triglochinin. J Chem Soc Chem Comm 1972:572–573

Ferdelman TG, Church TM, Luther GW III (1991) Sulfur enrichment of humic substances in a Delaware salt marsh sediment core. Geochim Cosmochim Acta 55:979–988

Gensemer RW, DeForest DK, Stenhouse AJ, Higgins CJ, Cardwell RD (2006) In: Dzombak DA, Ghosh RS, Wong-Chong GM (eds) Cyanide in water and soil. CRC Press, Boca Raton, pp 251–284

Ghosh RS, Meeussen JCL, Dzombak DA, Nakles DV (2006a) In: Dzombak DA, Ghosh RS, Wong-Chong GM (eds) Cyanide in water and soil. CRC Press, Boca Raton, pp 191–208

Ghosh RS, Ebbs SD, Bushey JT, Neuhauser EF, Wong-Chong GM (2006b) In: Dzombak DA, Ghosh RS, Wong-Chong GM (eds) Cyanide in water and soil. CRC Press, Boca Raton, pp 225–236

Kamyshny A Jr (2009) Improved cyanolysis protocol for detection of zero-valent sulfur in natural aquatic systems. Limnol Oceanogr Meth 7:442–448

Kamyshny Jr A, Oduro H, Farquhar J (2012) Quantification of free and metal-complexed cyanide by tetrathionate derivatization. Int J Environ Anal Chem, (in print), doi:10.1080/03067319.2011.561339

Kamyshny A Jr, Borkenstein CG, Ferdelman TG (2009) Protocol for quantitative detection of elemental sulfur and polysulfide zero-valent sulfur distribution in natural aquatic samples. Geostand Geoanal Res 33:415–435

Kamyshny A Jr, Zerkle AL, Mansaray Z, Ciglenečki I, Bura-Nakić E, Farquhar J, Ferdelman TG (2011) Biogeochemical sulfur cycle in water column of shallow stratified sea-water lake: speciation and quadruple sulfur isotope composition. Mar Chem 127:144–154

Karavaiko GI, Kondrat'eva TF, Savari EE, Grigor'eva NV, Avakyan ZA (2000) Microbial degradation of cyanide and thiocyanate. Microbiology 69:167–173

Keefe AD, Miller SL (1996) Was ferrocyanide a prebiotic reagent? Orig Life Evol Biosphere 26:111–129

Kelly DP, Chambers LA, Trudinger PA (1969) Cyanolysis and spectrophotometric estimation of trithionate in mixture with thiosulfate and tetrathionate. Anal Chem 41:898–901
Kim YM, Park D, Jeon CO, Lee DS, Park JM (2008) Effect of HRT on the biological pre-denitrification process for the simultaneous removal of toxic pollutants from cokes wastewater. Bioresour Technol 99:8824–8832
Knowles CJ (1976) Microorganisms and cyanide. Bacteriol Rev 40:652–680
Kostka JE, Luther GW (1994) Partitioning and speciation of solid phase iron in saltmarsh sediments. Geochim Cosmochim Acta 58:1701–1710
Kostka JE, Luther GW (1995) Seasonal cycling of Fe in saltmarsh sediments. Biogeochemistry 29:159–181
Li Q, Jacob DJ, Bey I, Yantosca RM, Zhao Y, Kondo Y, Notholt J (2000) Atmospheric hydrogen cyanide (HCN): biomass burning source, ocean sink? Geophys Res Lett 27:357–360
Lord CJ III, Church TM (1983) The geochemistry of salt marshes: sedimentary ion diffusion, sulfate reduction, and pyritization. Geochim Cosmochim Acta 47:1381–1391
Luther GW III, Church TM, Scudlark JR, Cosman M (1986) Inorganic and organic sulfur cycling in salt-marsh pore waters. Science 232:746–749
Luther GW III, Ferdelman TG, Kostka JE, Tsamakis EJ, Church TM (1991) Temporal and spatial variability of reduced sulfur species (FeS_2, $S_2O_3^{2-}$) and porewater parameters in salt marsh sediments. Biogeochemistry 14:57–88
Luthy RG, Bruce SG Jr (1979) Kinetics of reaction of cyanide and reduced sulfur species in aqueous solutions. Environ Sci Technol 13:1481–1487
Majak W, McDiarmid RE, Hall JW, Van Ryswyk AL (1980) Seasonal variation in the cyanide potential of arrowgrass (*Triglochin maritima*). Can J Plant Sci 60:1235–1241
Meeussen JCL, Keizer MG, de Haan FAM (1992) Chemical stability and decomposition rate of iron cyanide complexes in soil solutions. Environ Sci Technol 26:511–516
Rong L, Lim LW, Takeuchi T (2005) Determination of iodide and thiocyanate in seawater by liquid chromatography with poly(ethylene glycol) stationary phase. Chromatographia 61:371–374
Sahariah BP, Saswati C (2011) Kinetic analysis of phenol, thiocyanate and ammonia-nitrogen removals in an anaerobic-anoxic-aerobic moving bed bioreactor system. J Hazard Mater 190:260–267
Seeberg-Elverfeldt J, Schlüter M, Feseker T, Kölling M (2005) Rhizon sampling of porewaters near the sediment-water interface of aquatic systems. Limnol Oceanogr Methods 3:361–371
Sekerka I, Lechner JF (1976) Potentiometric determination of low levels of simple and total cyanides. Water Res 10:479–483
Shieh WK, Richards DJ (1988) Anoxic/oxic activated sludge treatment kinetics of cyanides and phenols. J Environ Eng-ASCE 114:639–654
Stratford J, Dias AEXO, Knowles CJ (1994) The utilization of thiocyanate as a nitrogen source by a heterotrophic bacterium: the degradative pathway involves formation of ammonia and tetrathionate. Microbiology 140:2657–2662
Szekeres L (1974) Analytical chemistry of sulfur acids. Talanta 21:1–44
Wild SR, Rudd T, Neller A (1994) Fate and effects of cyanide during wastewater treatment processes. Sci Total Environ 156:93–107
Wong-Chong GM, Dzombak DA, Gjosh RS (2006a) In: Dzombak DA, Ghosh RS, Wong-Chong GM (eds) Cyanide in water and soil. CRC Press, Boca Raton, pp 1–14
Wong-Chong GM, Ghosh RS, Bushey JT, Ebbs SD, Neuhauser EF (2006b) In: Dzombak DA, Ghosh RS, Wong-Chong GM (eds) Cyanide in water and soil. CRC Press, Boca Raton, pp 25–40
Wood AP, Kelly DP, McDonald IR, Jordan SL, Morgan TD, Khan S, Murrell JC, Borodina E (1998) A novel pink-pigmented facultative methylotroph, *Methylobacterium thiocyanatum* sp. nov., capable of growth on thiocyanate or cyanate as sole nitrogen sources. Arch Microbiol 169:148–158
Yao W, Millero FJ (1993) The rate of sulfide oxidation by δMnO2 in seawater. Geochim Cosmochim Acta 57:3359–3365
Yao W, Millero FJ (1996) Oxidation of hydrogen sulfide by hydrous Fe(III) oxides in seawater. Mar Chem 52:1–16
Young TC, Zhao X, Theis TL (2006) In: Dzombak DA, Ghosh RS, Wong-Chong GM (eds) Cyanide in water and soil. CRC Press, Boca Raton, pp 171–190
Yu X, Zhou P, Xishi Z, Liu Y (2005) Cyanide removal y Chinese vegetation—quantification of the Michaelis-Menten kinetics. Environ Sci Pollut Res 12:221–226
Zopfi J, Böttcher ME, Jørgensen BB (2008) Biogeochemistry of sulfur and iron in *Thioploca*-colonized surface sediments in the upwelling area off central Chile. Geochim Cosmochim Acta 72:827–843